ACS Sustainable Chemistry & Engineering

Research Article

pubs.acs.org/journal/ascecg

Molybdenum Carbide Anchored on Graphene Nanoribbons as Highly Efficient All-pH Hydrogen Evolution Reaction Electrocatalyst

Wei Gao,[†] Yiqin Shi,[‡] Youfang Zhang,[†] Lizeng Zuo,[†] Hengyi Lu,[†] Yunpeng Huang,[†] Wei Fan,*[,‡] and Tianxi Liu*[,†,‡]

[†]State Key Laboratory of Molecular Engineering of Polymers, Department of Macromolecular Science, Fudan University, 220 Handan Road, Shanghai 200433, P. R. China

[‡]State Key Laboratory for Modification of Chemical Fibers and Polymer Materials, College of Materials Science and Engineering, Donghua University, 2999 North Renmin Road, Shanghai 201620, P. R. China

Supporting Information

ABSTRACT: The demand for exploiting hydrogen as a new energy source has driven the development of feasible, efficient, and low-cost electrocatalysts for hydrogen evolution reaction (HER) in different reaction media. Herein, we report the synthesis of molybdenum carbide (Mo_2C) nanoparticles anchored on graphene nanoribbons (GNRs) as HER electrocatalyst that can function well under acidic, basic, and neutral conditions. GNRs obtained by unzipping carbon nanotubes (CNTs) display strip-like structure, offering abundant active sites for growing Mo_2C nanoparticles. Furthermore, GNRs could provide a fast electron transport pathway as well as large exposed surface area to allow full impregnation of electrolytes. Coupling with the anticorrosion feature of Mo_2C nanoparticles, the Mo_2C−GNR hybrid exhibits outstanding electrocatalytic performance in all of the acidic, basic, and neutral media, making it promising as a highly efficient electrocatalyst under conditions at all pH values.

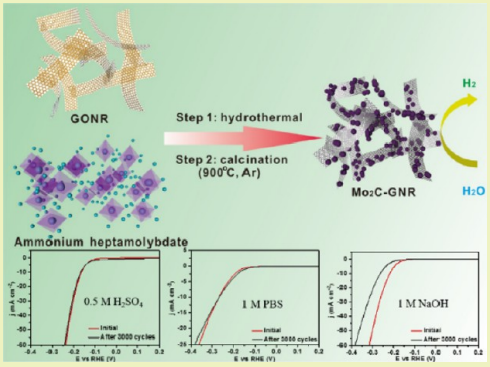

KEYWORDS: *Molybdenum carbide, Graphene nanoribbons, All-pH value, Hydrogen evolution reaction, Electrocatalyst*

INTRODUCTION

The increasing demand for alternative and renewable energy sources to replace the exhaustible fossil fuels has prompted the exploitation of hydrogen, a potential energy carrier in the future. The evolution of hydrogen through splitting water has attracted a lot of attention, and to achieve hydrogen in a greener and more sustainable way compared with current industrial production, optimal electrocatalytic materials are ceaselessly being explored.[1] Furthermore, besides developing common hydrogen evolution reaction (HER) catalysts that work well in the acidic environment, many water−alkali electrolyzers need catalysts to operate actively and durably in a basic environment to couple with the oxygen evolution reaction, while many microbial electrolysis cells need catalysts which can function well in neutral media.[2] Therefore, manufacturing HER electrocatalysts that can operate under all pH values is intensively investigated.[3−5]

Since the high-cost of currently adopted noble metal catalysts greatly limits the scalability of practical applications, many efforts have been exerted to develop inexpensive and earth-abundant transition metal compounds as promising catalysts for HER.[6,7] Among them, transition metal carbides, especially molybdenum carbide (Mo_2C), due to the similar electronic density of state of the d-band to that of Pt together with excellent hydrogen adsorption activity, are favorable for efficient HER electrocatalysis.[8,9] And in the solutions over all pH ranges, oxide species can be formed on the surface of Mo_2C and could kinetically limit the corrosion of electroactive materials, assuring its stability as all-pH HER electrocatalyst.[10] However, bare Mo_2C nanoparticles possess drawbacks, such as poor processability[11] and easy aggregation, which lead to decrease of active sites, thus impeding the improvement of the electrocatalytic effect. Various strategies, including nanostructuring,[12,13] introduction of dopants,[14] and hybridization with supporting materials,[10,15,16] have been applied to increase the density of active sites. Carbon nanomaterials, such as carbon nanotubes (CNTs),[17] porous carbon,[18] graphitic carbon sheets,[15] and carbon cloth,[19] have been previously reported as templates for growing Mo_2C nanoparticles in the utilization of high electrical conductivity and large surface area. Graphene nanoribbons (GNRs), obtained by longitudinally unzipping CNTs, not only inherit high electrical conductivity from CNTs, but also possess straight edge sites and high aspect ratios with no significant shortening of the parent tubes.[20] Therefore, GNRs have been evidenced to be prominent building blocks to construct high-performance dye-sensitized solar cells,[21] supercapacitors,[22] oxygen reduction reaction electrocatalysts,[23] and HER electrocatalysts.[24]

Received: April 25, 2016
Revised: September 22, 2016
Published: October 10, 2016

DOI: 10.1021/acssuschemeng.6b00859
ACS Sustainable Chem. Eng. 2016, 4, 6313−6321

Scheme 1. Schematic Illustration for the Preparation of Mo_2C−GNR Hybrids

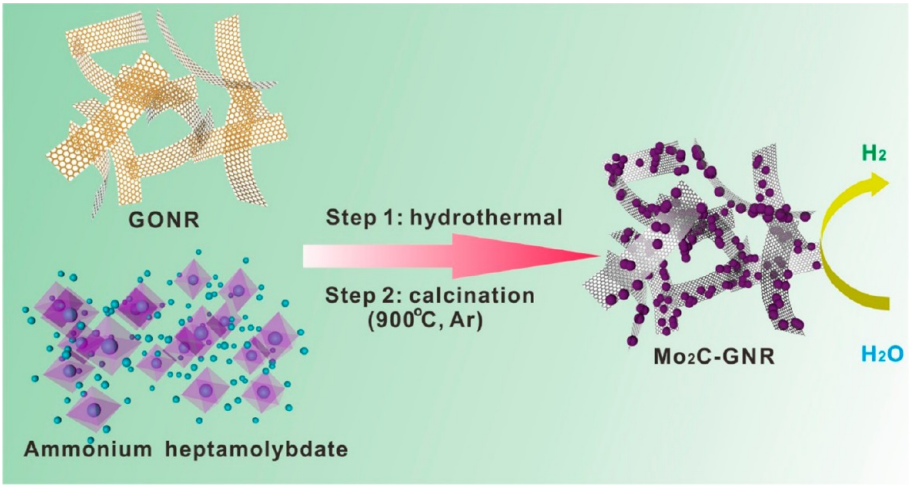

In this work, we are the first to use GNRs as templates for the *in situ* growth of carbides, and hierarchically structured Mo_2C−GNR hybrids were fabricated by a hydrothermal method followed by calcination. In this process, glucose is used as both carbon source and stabilizing agent.[25] In this hybridized structure, quasi-one-dimensional GNRs with open structure could evenly and densely anchor Mo_2C nanoparticles on both of the edges and surface planes, enabling the exposure of abundant active sites for electrocatalysis. The interconnected GNR network provides conductive pathways for fast electron transport and large accessible surface area for full contact with electrolyte. The HER performance of Mo_2C−GNR hybrids is investigated in acidic, basic, and neutral media, respectively. And this strategy of coupling metal carbides with GNRs can be extended to other electrochemical applications.

EXPERIMENTAL SECTION

Materials. Multiwalled carbon nanotubes (MWCNTs) (diameter: 30−50 nm) were obtained from Chengdu Organic Chemicals Co. Ltd., synthesized by the chemical vapor deposition method. H_2SO_4 (95−98%), H_3PO_4 (85%), H_2O_2 (30%), *N*,*N*-dimethylformamide (DMF, ≥99.5%), ethanol, glucose, potassium permanganate ($KMnO_4$), and ammonium molybdate ($(NH_4)_6Mo_7O_{24}{\cdot}4H_2O$) were purchased from Sinopharm Chemical Reagent Co., Ltd. Deionized (DI) water was used throughout all the experiments.

Preparation of Graphene Oxide Nanoribbons (GONRs). GONRs were prepared by longitudinally unzipping MWCNTs through a simple solution-based oxidative process.[26] Typically, 150 mg of pristine MWCNTs was dispersed in 36 mL of H_2SO_4, and stirred for 1 h to form a homogeneous dispersion. Then, 7 mL of H_3PO_4 was added dropwise and stirred for another 30 min. 750 mg of $KMnO_4$ was gradually added, and the mixture was kept under reaction at 70 °C for 2 h. After naturally being cooled down to room temperature, the mixture was poured into 150 mL of ice water containing 7 mL of H_2O_2. The products were allowed to coagulate overnight, and the precipitates were washed with 10% HCl, followed by washing with ethanol/ether several times. Finally, the suspension was centrifuged to obtain the solid products.

Preparation of Molybdenum Carbide−Graphene Nanoribbon (Mo_2C−GNR) Hybrids. Mo_2C−GNR hybrids were prepared as illustrated in Scheme 1. First, 40 mg of the as-obtained GONRs was dispersed in 20 mL of H_2O to form a 2 mg mL^{-1} dispersion. A certain amount of $(NH_4)_6Mo_7O_{24}{\cdot}4H_2O$ and glucose with weight ratio of 4:1 was dissolved in 20 mL of H_2O, then blended with the above GONRs dispersion, and kept under stirring for 30 min, and the mixture was subsequently transferred into a 100 mL Teflon stainless-steel autoclave and reacted at 180 °C for 12 h. The precipitates were collected through centrifugation with a speed of 10000 rpm for 10 min, followed by repeatedly washing with DI water and ethanol, and finally dried under 60 °C overnight. Afterward, the samples were carbonized at 900 °C under argon atmosphere for 2 h with a heating rate of 5 °C min^{-1} to get the final products. The Mo_2C−GNR hybrids obtained with initial $(NH_4)_6Mo_7O_{24}{\cdot}4H_2O$ addition of 100, 200, and 400 mg were denoted as Mo_2C−GNR-1, Mo_2C−GNR-2, and Mo_2C−GNR-3, respectively.

For comparison, bare Mo_2C nanoparticles were prepared through the same procedure without the addition of GONRs, and pure GNRs were prepared by direct carbonization of GNORs. Besides, Mo_2C−CNT hybrid was fabricated by replacing GONRs with acid-treated CNTs in the precursor.

Characterizations. The morphology of samples was characterized by field emission scanning electron microscopy (FESEM) (Ultra 55, Zeiss) at an acceleration voltage of 5 kV. The chemical composition was characterized by energy dispersive X-ray spectroscopy (EDX). Transmission electron microscopy (TEM) observations were performed with a JEOL JEM 2100 TEM under an acceleration voltage of 200 kV. Samples for TEM observations were prepared by dropping solutions on the copper grids and drying in the air. X-ray diffraction (XRD) patterns were obtained on an X'Pert Pro X-ray diffractometer with Cu Kα radiation (λ = 0.1542 nm) under a current of 40 mA and a voltage of 40 kV with 2θ ranges from 5° to 80°. Raman spectra were conducted on a JobinYvon XploRA Raman spectrometer at an exciting wavelength of 632.8 nm. X-ray photoelectron spectroscopy (XPS) analyses were conducted with a VG ESCALAB 220I-XL device, and all XPS spectra were corrected using the C 1s line at 284.5 eV. In addition, the curve fitting and background subtraction were accomplished using XPS PEAK41 software. The specific surface area and pore size distribution were characterized with a belsorp-max surface area detecting instrument (Tristar3000) by N_2 physisorption at 77 K. Thermogravimetric analysis (Pyris 1 TGA) was performed under air flow from 100 to 800 °C at a heating rate of 20 °C min^{-1}.

Electrochemical Measurements. Prior to all the hydrogen evolution experiments, glassy carbon electrodes (GCE) (diameter: 3 mm) were pretreated according to the previous report.[27] The working electrode was prepared as follows: 2 mg of Mo_2C−GNR hybrid was dispersed in 1 mL of DMF/DI water mixed solution (volume ratio: 1:3) containing 20 μL of 5 wt % nafion. Then, the mixture was sonicated for 2 h to obtain the homogeneous slurry. Finally, 10 μL of the slurry was dropped onto GCE and dried at room temperature to achieve Mo_2C−GNR hybrid modified GCE.

All electrochemical catalytic tests were performed with a standard three-electrode CHI 660D electrochemical workstation (Chenhua Instruments Co, Shanghai, China) at room temperature, where sample modified GCE was applied as the working electrode, with a saturated

DOI: 10.1021/acssuschemeng.6b00859
ACS Sustainable Chem. Eng. 2016, 4, 6313−6321

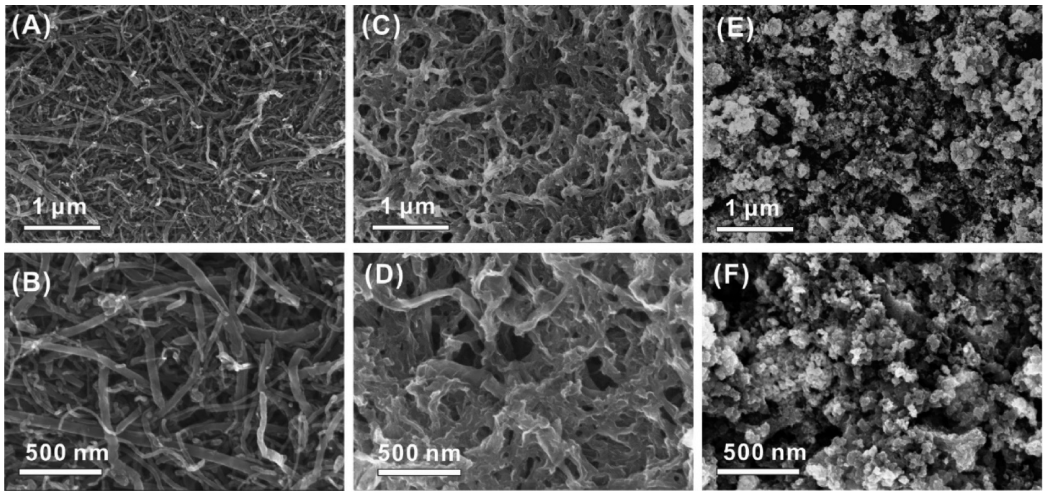

Figure 1. SEM images of (A, B) CNTs, (C, D) GONRs, and (E, F) bare Mo_2C nanoparticles at low and high magnifications.

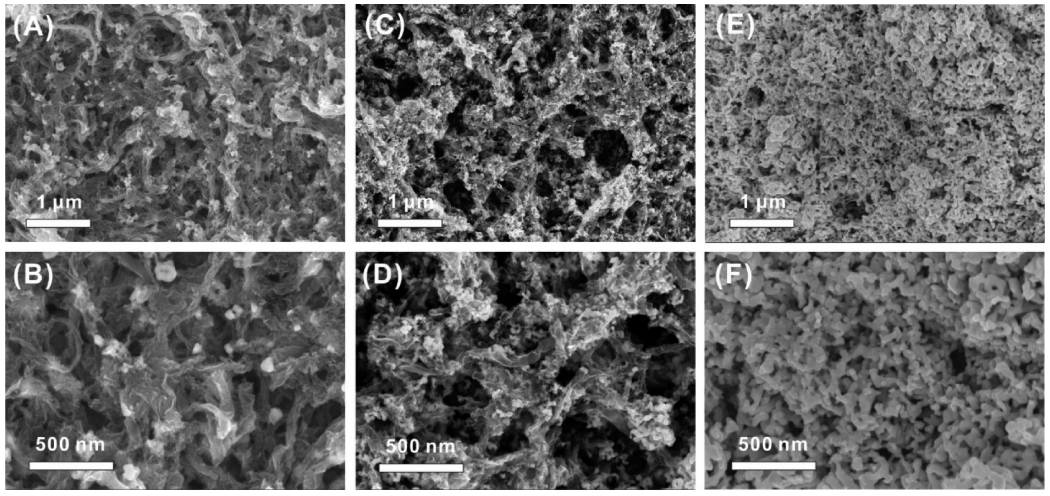

Figure 2. SEM images of Mo_2C−GNR hybrids with different loadings of Mo_2C: (A, B) Mo_2C−GNR-1; (C, D) Mo_2C−GNR-2; (E, F) Mo_2C−GNR-3.

calomel electrode (SCE) as the reference electrode and Pt wire as counter electrode. The hydrogen evolution performance tests of the Mo_2C−GNR hybrid were performed by linear sweep voltammetry (LSV) in a nitrogen purged electrolyte solution of 0.5 M H_2SO_4, 1 M NaOH, and 1 M PBS, respectively, with a scan rate of 2 mV s^{-1}. The cycling stability was investigated by cyclic voltammetry (CV) between −0.35 and 0.25 V vs RHE at a scan rate of 100 mV s^{-1}. In our electrochemical tests, all the potentials were calibrated to RHE according to the equation $E_{RHE} = E_{SCE} + (0.241 + 0.059\ pH)$ V.

RESULTS AND DISCUSSION

Morphology and Structure of Mo_2C−GNR Hybrids. Through the oxidative unzipping method, pristine MWCNTs with closed tubular structure were transformed into layered GONR sheets (Figure 1A−1D). And after the longitudinally unzipping, strip-like GONRs retain the length feature of MWCNTs while possessing higher aspect ratios, verifying that they were unzipped successfully (Figure S1A, S1B). Compared with pristine MWCNTs, GONRs present a larger surface area of approximate 78 $m^2\ g^{-1}$ and a mesopore size of about 3 nm (Figure S2), as well as more functional groups for anchoring Mo_2C nanoparticles. Furthermore, the open structure renders more interfacial contact with the electrolyte. All these advantages of GONRs can benefit the HER performance when serving as carbon supports for the catalytic hybrid materials. Without any templates for growing, bare Mo_2C nanoparticles tend to form aggregates with random morphology (Figure 1E, F). The conglutination between nanoparticles could reduce electrocatalytic active sites as well as hindering the impregnation of electrolyte. To solve these problems derived from severe aggregation of bare Mo_2C nanoparticles, GONRs are used as supporting materials for anchoring and miniaturization of Mo_2C nanoparticles to improve the effective surface area and thus the catalytic activity. In the experiment, glucose is used as carbon source. Without the addition of glucose, Mo_2C nanoparticles are formed by consuming the carbon from GONRs and can hardly be immobilized on the surface of GNRs (Figure S3). By tuning the added amount of $(NH_4)_6Mo_7O_{24}\cdot 4H_2O$ in the precursor, Mo_2C−GNR-1, Mo_2C−GNR-2, and Mo_2C−GNR-3 are prepared with different loadings of Mo_2C nanoparticles. With less addition of $(NH_4)_6Mo_7O_{24}\cdot 4H_2O$, as in Mo_2C−GNR-1, Mo_2C nanoparticles are sparsely decorated on GNRs surface, and most of the area of the GNRs surface is uncovered (Figure 2A, 2B). With moderate added amount of $(NH_4)_6Mo_7O_{24}\cdot 4H_2O$, in the formed Mo_2C−GNR-2 hybrid, Mo_2C nanoparticles are evenly anchored on the three-dimensional network of GNRs with a fine coverage (Figure

DOI: 10.1021/acssuschemeng.6b00859
ACS Sustainable Chem. Eng. 2016, 4, 6313−6321

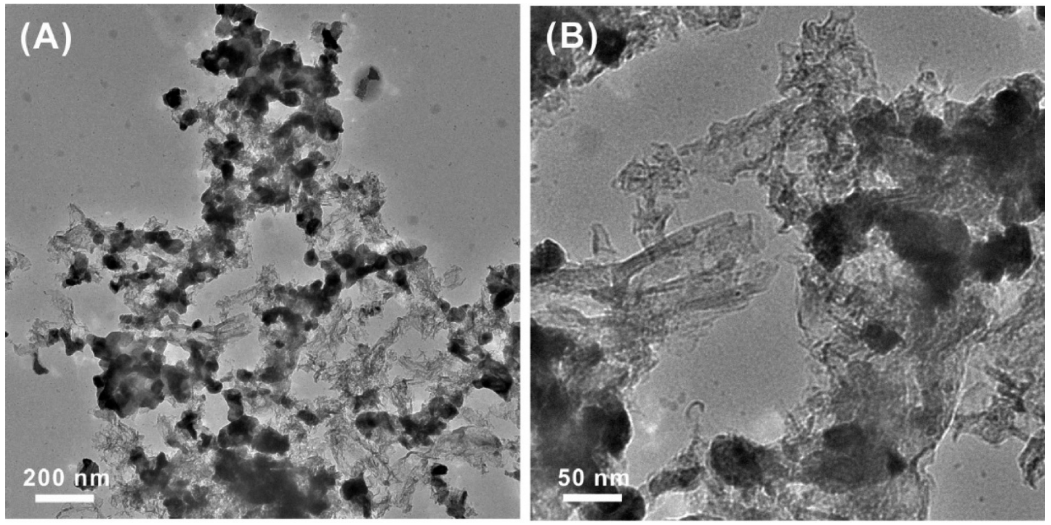

Figure 3. TEM images of Mo_2C−GNR-2 at (A) low and (B) high magnifications.

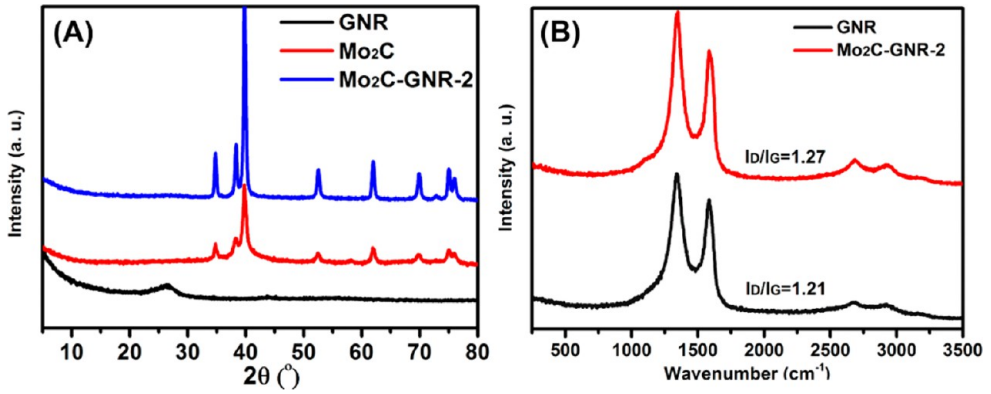

Figure 4. (A) XRD patterns of GNR, pure Mo_2C, and Mo_2C−GNR-2 hybrid. (B) Raman spectra of GNR and Mo_2C−GNR-2 hybrid.

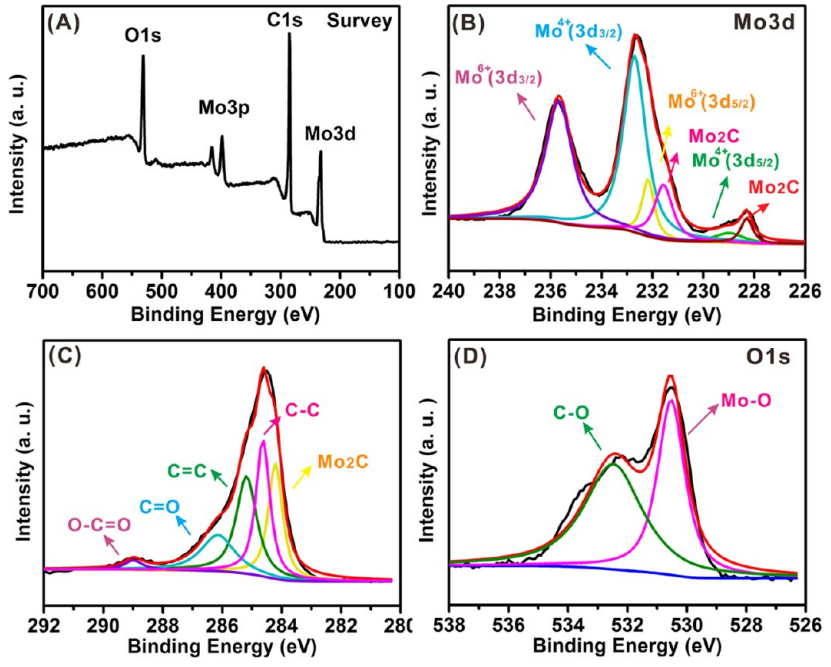

Figure 5. XPS spectra of the Mo_2C−GNR-2 hybrid: (A) survey spectrum; high-resolution (B) Mo 3d, (C) C 1s, and (D) O 1s spectra.

DOI: 10.1021/acssuschemeng.6b00859
ACS Sustainable Chem. Eng. 2016, 4, 6313−6321

2C, D). In distinct comparison, under the same reaction conditions, acid-treated MWCNTs immobilize much less Mo_2C nanoparticles due to the less functional groups bonded surface and closed tubular structure (Figure S4). As the added amount of $(NH_4)_6Mo_7O_{24}{\cdot}4H_2O$ further increases, GNRs can hardly be observed in the hybrid and the overloading of Mo_2C nanoparticles leads to severe agglomeration, causing loss of exposed active edges (Figure 2E, F). From the EDX results taken from Mo_2C−GNR-2 (Figure S5), Mo_2C nanoparticles are further confirmed to have a uniform distribution on GNRs. And after the high-temperature calcination at 900 °C under inert atmosphere, most of the oxygen-containing species are removed, as indicated by the low oxygen content in Figure S5B. From the TEM images and high-magnification SEM image of Mo_2C−GNR-2, the strip-like structures of GNRs are well maintained in the hybrid, offering sites for anchoring Mo_2C nanoparticles with average size of approximately 50 nm (Figure 3, Figure S6).

From the XRD patterns of GNR and bare Mo_2C and Mo_2C−GNR-2, it is clearly seen that GNR displays a broad peak centered at $2\theta = 26.4°$, which is assigned to the (002) plane of the stacked GNR layer. Those sharp peaks of carbonized bare Mo_2C and Mo_2C−GNR-2 hybrid are consistent with the reference XRD patterns of hexagonal β-Mo_2C (JCPSD No. 00-035-0787) (Figure 4A), which is the most active phase for HER electrocatalysis among the four phases of molybdenum carbide.[28−30] The absence of peaks from byproducts indicates the synthetic method employed is very effective in preparing pure Mo_2C on GNRs. In the supplement of XRD patterns, the Raman spectrum of Mo_2C−GNR-2 is tested and shows two well-documented bands, the D band at 1338 cm^{-1} and the G band at 1580 cm^{-1}, corresponding to disordered carbon and the E_g vibration of sp^2 bonded carbon atoms, respectively, which is similar to the case of pure GNR but with different intensity ratio (I_D/I_G) (Figure 4B).

The composition and surface chemical state of the Mo_2C−GNR hybrid are analyzed by XPS. From the survey spectrum of Mo_2C−GNR-2, C, O, and Mo are observed as the main elements coexisting in the hybrid (Figure 5A). The high-resolution spectra of Mo 3d can be deconvoluted into three doublets (Figure 5B).[31] One doublet centered at 228.3 and 231.6 eV indicates the presence of Mo_2C, and two peaks at 229.0 and 232.7 eV can be attributed to Mo^{4+} in MoO_2. Doublets centered at 235.7 and 232.2 eV are observed for Mo^{6+} $3d_{3/2}$ and Mo^{6+} $3d_{5/2}$, respectively, which is probably caused by the oxidation of Mo during the XPS test at high energy when exposed to air. The high-resolution XPS spectrum of C 1s is shown in Figure 5C, whereas peaks at 284.5, 285.2, 286.2, and 289.0 eV correspond to C−C bonds and oxygen-containing C−O, C═O, and O−C═O bonds, respectively. Additionally, the peak at lower binding energy of 284.2 eV belongs to molybdenum bonded carbon.[31] In the high-resolution O 1s spectrum, these two split peaks at 530.5 and 532.5 eV represent Mo−O bonds and C−O bonds, respectively (Figure 5D).

TGA tests have been carried out to quantify the loading amount of Mo_2C on carbon support (Figure S7). A previous report has revealed the final product of Mo_2C after TGA analysis is MoO_3. The chemical reaction of Mo_2C being converted into oxides under heating in air atmosphere can be depicted as the following:[32]

$$Mo_2C + 4O_2 = 2MoO_3 + CO_2$$

On the basis of residue MoO_3 contents and the above equation, the loading amount of Mo_2C catalysts on carbon support evaluated from TGA results is 21.9, 49.4, and 89.6 wt % for Mo_2C−GNR-1, Mo_2C−GNR-2, and Mo_2C−GNR-3, respectively. The contents of Mo_2C increase as the initial addition amount of ammonium molybdate and glucose in the precursor solution increases, which accords well with the SEM images in Figure 2.

HER Electrocatalytic Activity of Mo_2C−GNR Hybrids. The electrocatalytic HER activities of Mo_2C−GNR hybrids were investigated using a three-electrode setup in electrolyte of 0.5 M H_2SO_4, 1 M NaOH, and 1 M PBS, respectively. To uncover the interplay between the loading of Mo_2C and the electrocatalytic activity, Mo_2C−GNR-1, Mo_2C−GNR-2, and Mo_2C−GNR-3 prepared with different loading amounts of Mo_2C were all measured for the HER performance in acidic solution, and the corresponding LSV curves are presented in Figure 6. Before the measurements, activation of the electrodes

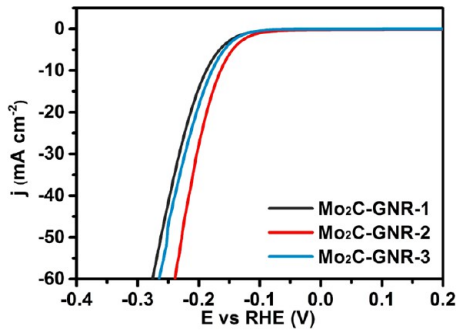

Figure 6. LSV polarization curves of Mo_2C−GNR-1, Mo_2C−GNR-2, and Mo_2C−GNR-3 modified GCE in N_2-purged 0.5 M H_2SO_4 solution. Scan rate: 2 mV s^{-1}.

was carried out through electrolysis for 10 min at 10 mA cm^{-2} to eliminate those catalytic-inactive oxides on the surface of Mo_2C. It is obvious that, among all these hybrids, Mo_2C−GNR-2 presents optimal HER catalytic activity, since the current density increases most rapidly with the smallest onset potential, indicating that it can evolve more hydrogen at lower potential. In view of the fact that the electrocatalytic behavior of the hybrid directly correlates with the number of catalytic active sites, Mo_2C−GNR-2, with Mo_2C nanoparticles densely distributed on the GNRs surface, provides much more abundant active catalytic sites than Mo_2C−GNR-1. And for Mo_2C−GNR-3, the aggregation of Mo_2C nanoparticles resembles the bulk Mo_2C, reducing the exposure of active sites to electrolyte. Proper loading of Mo_2C nanoparticles on GNRs surface could facilitate the full utilization of active sites of catalyst and rapid electron transport simultaneously. And this anchoring configuration induces negative charge transfer from molybdenum to carbon, which can decrease the hydrogen binding energy by downshifting the d-band center of molybdenum. This favors the electrochemical desorption of H atoms and results in a moderate Mo−H binding strength, leading to enhanced HER performance.[8]

HER performances were also measured and compared between Mo_2C−GNR-2, bare Mo_2C, GNR, Mo_2C−CNT, and Pt (Figure 7A). GNR exhibits almost no electrocatalytic activity, while bare Mo_2C and Mo_2C−CNT prepared through the same procedure as Mo_2C−GNR-2 display a distinct catalytic effect toward HER, and the hybrid of Mo_2C−GNR-

DOI: 10.1021/acssuschemeng.6b00859
ACS Sustainable Chem. Eng. 2016, 4, 6313−6321

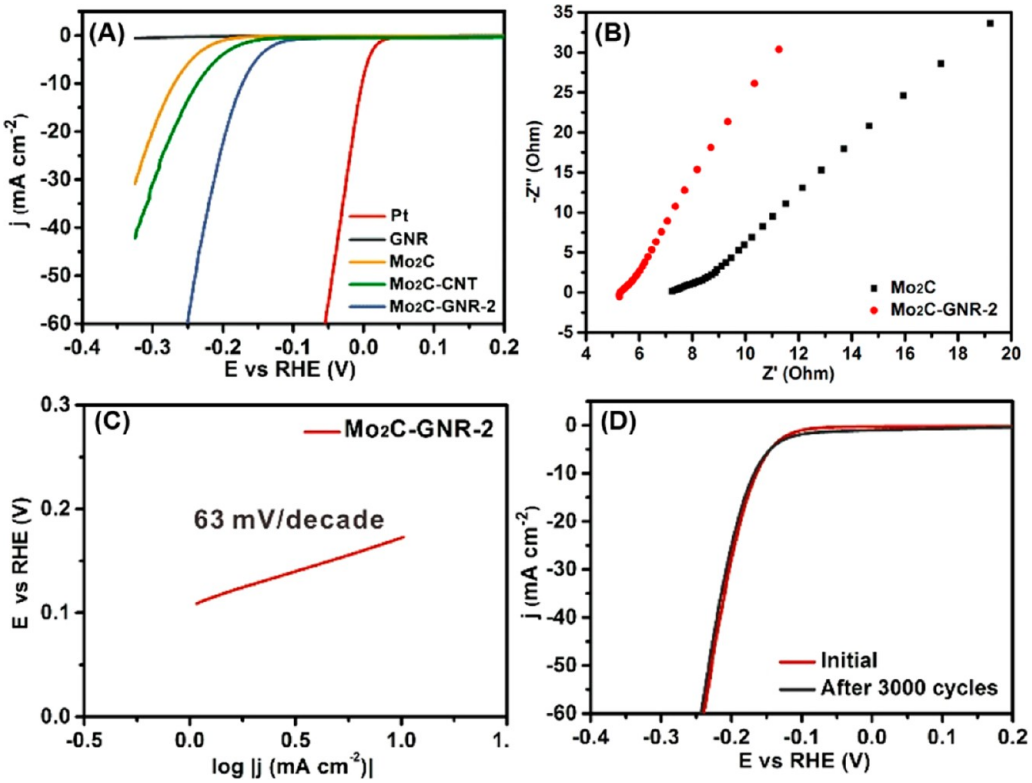

Figure 7. (A) LSV polarization curves of Pt, GNR, Mo_2C, Mo_2C−CNT, and Mo_2C−GNR-2 modified GCE in N_2-purged 0.5 M H_2SO_4 solution. (B) Nyquist plots of pure Mo_2C and Mo_2C−GNR-2. (C) Tafel plot of Mo_2C−GNR-2 modified GCE. (D) LSV polarization curves for Mo_2C−GNR-2 modified GCE recorded before and after 3000 times of CV cycles.

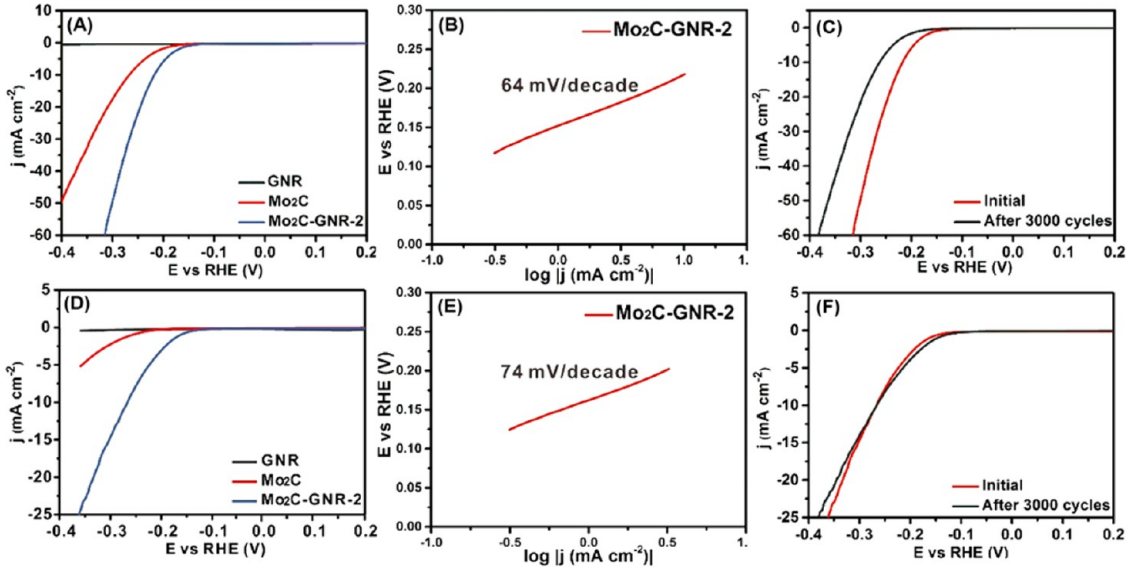

Figure 8. (A) LSV polarization curves of GNR, Mo_2C, and Mo_2C−GNR-2 modified GCE in N_2-purged 1 M NaOH solution and corresponding (B) Tafel plots and (C) LSV polarization curves of Mo_2C−GNR-2 recorded before and after 3000 times of CV cycles. (D) LSV polarization curves of GNR, Mo_2C, and Mo_2C−GNR-2 modified GCE in N_2-purged 1 M PBS solution and corresponding (E) Tafel plots and (F) LSV polarization curves of Mo_2C−GNR-2 recorded before and after 3000 times of CV cycles. Scan rate of LSV polarization curves: 2 mV s^{-1}.

2 displays much lower onset potential (100 mV) and higher current density, affording a current density of 10 mA cm^{-2} at a relative low overpotential of 167 mV. The improved catalytic activity can be attributed to the hybrid structure, in which GNRs function as supporting materials, inhibiting agglomeration of Mo_2C, which greatly hinders the catalytic performance. Moreover, compared with tubular CNTs,[33,34] the open structure of GNRs shows more advantages in anchoring Mo_2C nanoparticles and enables more favorable permeation of electrolyte into the hybrid. As a result, the hybrid gains larger electrochemically active surface area (ECSA) (76.9 cm^2 calculated for Mo_2C−GNR-2) than individual components (9.5 cm^2 for GNR, 33.9 cm^2 for Mo_2C), indicating more electroactive material could be exposed to the electrolyte

DOI: 10.1021/acssuschemeng.6b00859
ACS Sustainable Chem. Eng. 2016, 4, 6313−6321

(Figure S8). Electrochemical impedance spectroscopy (EIS) analysis has been carried out to study the transport kinetics of electrodes. Observed from the Nyquist plots presented in Figure 7B, Mo_2C−GNR exhibits a smaller semicircle diameter in the high-frequency region and a more vertical line in the low-frequency range compared with pure Mo_2C, revealing that the hybrid affords lower impedance and markedly faster HER kinetics, as the presence of GNR could enhance the conductivity of the catalytic electrodes. To gain further insight into the catalytic activity of the Mo_2C−GNR hybrid, the slope is extracted from Tafel plots (Figure 7C) with the equation of $\eta = b \log j + a$, where η is the overpotential, b is the Tafel slope, j is the current density, and a is the intercept. The Tafel slope for Mo_2C−GNR-2 is calculated to be 63 mV decade^{-1}. This value demonstrates that Mo_2C−GNR-2 catalyzed HER proceeds by a Volmer−Heyrovsky mechanism, where a two-step process takes place: the rapid discharge step (the Volmer reaction) comes first with a following rate-limiting electrochemical desorption step (the Heyrovsky reaction). The durability of Mo_2C−GNR-2 electrocatalyst in the acidic solution was studied before and after scanning 3000 cyclic voltammetry (CV) cycles from −0.35 to 0.25 V (vs RHE) with a scan rate of 100 mV s^{-1} (Figure 7D). It is observed that, after the cycling procedure, Mo_2C−GNR-2 presents similar LSV curves to the initial cycle with ignorable cathodic current loss, demonstrating that the hybrid is very stable under acidic experimental conditions.

To verify the electrocatalytic activity of Mo_2C−GNR-2 under the tested conditions over the whole pH range, 1 M NaOH and 1 M neutral PBS (pH = 7) solutions were also used as electrolytes for HER tests. It is clearly seen in basic media that the hybrid exhibits better HER performance than GNR and bare Mo_2C nanoparticles, as in acidic environment. An onset potential of 116 mV and a Tafel slope of 64 mV decade^{-1} are obtained, and for driving a cathodic current density of 10 mA cm^{-2}, a relatively low overpotential of 217 mV is required (Figure 8A, B). To assess the stability in alkaline media, 3000 CV cycles were run and the LSV curve after cycling has a negative shift compared with the initial one (Figure 8C). Although the Mo_2C−GNR-2 hybrid does not present stability as good as in the acidic environment, this degradation of activity is in the acceptable range. Neutral media are generally preferred to perform electrocatalytic reactions, since they are more benign than acidic and basic environments, and less corrosion or oxidation of electrocatalysts will occur under this condition. In the neutral PBS solution, due to the inherently slow kinetics of HER in neutral electrolytes, electrocatalytic activity is not as good as that in H_2SO_4 or NaOH. However, Mo_2C−GNR-2 still presents a small onset potential of 124 mV, with an estimated Tafel slope of 74 mV decade^{-1} and a driving overpotential of 266 mV for the current density of 10 mA cm^{-2}, which is greatly enhanced compared with GNR and Mo_2C (Figure 8D, E). In neutral media, the Mo_2C−GNR-2 catalyst can be used with very little attenuation for 3000 cycles (Figure 8F). All these results demonstrate good electrocatalytic activity, surpassing or being comparable with most of the recently reported earth-abundant electrocatalysts (Table 1).[35−43] Compared with those pure Mo_2C nanocrystals such as Mo_2C nanoparticles[39] and nanowires,[13] the catalytic performance of the Mo_2C−GNR hybrid has been drastically improved due to the synergistic effect of Mo_2C and GNR. Furthermore, most of the recently developed earth-abundant HER electrocatalysts only work well under acidic conditions.[35−38] In contrast, Mo_2C−GNR can also operate under neutral and basic solutions, with a good performance compared with previous reports,[3,43] making it suitable to couple with OER in the same solution, thus addressing one of the main issues that plague water splitting reactions. Under conditions over the entire pH range, Mo_2C−GNR presents outstanding anticorrosion stability originating from the formation of surface oxide species.[44]

Table 1. Comparison of the HER Performance of Earth-Abundant Catalysts

Electrode materials	Current density (mA cm^{-2})	Potential vs RHE (V)	Tafel slope (mV dec^{-1})	ref
Co-FeS_2	10	120	56	35
CoPS	10	48	48	36
CoS_2	2	83		37
Mo_2C NWs	10.2	200	55.8	13
MoP/S	10	64		38
Mo_2C NPs	10	198		39
MoB	17	250	55	40
Mo_2C	19	250	56	40
$CoSe_2$	19	250	85	41
Cu_3P	10	143	67	42
Ni wire	10 (basic)	350		43
Co-NRCNTs	10 (neutral)	540		3
Mo_2C−GNR	10 (acidic)	167	63	This work
	10 (basic)	217	64	
	10 (neutral)	266	74	

CONCLUSIONS

In summary, Mo_2C nanoparticles anchored on GNRs have been prepared through hydrothermal synthesis and subsequent high-temperature calcination. The unique open structure of GNRs provides enlarged surface area for Mo_2C attachment and renders abundant active sites contacting with electrolyte. The optimal electron transfer pathway derived from the conductive network of GNRs coupling with the anticorrosion feature of Mo_2C endows the well-designed hybrid with effective and durable electrocatalytic activity for HER under conditions over all pH values. The strategy of in situ growing nanoparticles on the templates of highly conductive GNRs can be extended to fabricate other metal carbide hybrids with applications as promising water-splitting catalysts, lithium ion batteries, or supercapacitors.

ASSOCIATED CONTENT

Supporting Information

The Supporting Information is available free of charge on the ACS Publications website at DOI: 10.1021/acssuschemeng.6b00859.

TEM images of CNTs and GONR, nitrogen adsorption/desorption isotherm and pore size distribution of GNR, SEM images of Mo_2C−GNR prepared without adding glucose, of Mo_2C−CNT, and of Mo_2C−GNR-2 at high magnification, EDX results of Mo_2C−GNR, TGA analysis, and ECSA evaluation (PDF)

AUTHOR INFORMATION

Corresponding Authors

*(W. Fan) E-mail: weifan@dhu.edu.cn .

*(T. X. Liu) E-mail: txliu@fudan.edu.cn or txliu@dhu.edu.cn. Tel: +86-21-55664197. Fax: +86-21-65640293.

DOI: 10.1021/acssuschemeng.6b00859
ACS Sustainable Chem. Eng. 2016, 4, 6313−6321

Notes

The authors declare no competing financial interest.

■ ACKNOWLEDGMENTS

The authors are grateful for the financial support from the National Natural Science Foundation of China (51125011, 51433001).

■ REFERENCES

(1) Zou, X. X.; Zhang, Y. Noble Metal-Free Hydrogen Evolution Catalysts for Water Splitting. *Chem. Soc. Rev.* **2015**, *44*, 5148−5180.
(2) Subbaraman, R.; Tripkovic, D.; Strmcnik, D.; Chang, K.-C.; Uchimura, M. A.; Paulikas, P.; Stamenkovic, V.; Markovic, N. M. Highly Efficient Electrocatalytic Hydrogen Production by MoS_x Grown on Graphene-Protected 3D Ni Foams. *Science* **2011**, *334*, 1256−1260.
(3) Zou, X. X.; Huang, X. X.; Goswami, A.; Silva, R.; Sathe, B. R.; Mikmeková, E.; Asefa, T. Cobalt-Embedded Nitrogen-Rich Carbon Nanotubes Efficiently Catalyze Hydrogen Evolution Reaction at All pH Values. *Angew. Chem.* **2014**, *126*, 4461−4465.
(4) Gupta, S.; Patel, N.; Miotello, A.; Kothari, D. Cobalt-Boride: an Efficient and Robust Electrocatalyst for Hydrogen Evolution Reaction. *J. Power Sources* **2015**, *279*, 620−625.
(5) Feng, L.-L.; Li, G.-D.; Liu, Y.; Wu, Y.; Chen, H.; Wang, Y.; Zou, Y.-C.; Wang, D.; Zou, X. Carbon-Armored Co_9S_8 Nanoparticles as All-pH Efficient and Durable H_2-Evolving Electrocatalysts. *ACS Appl. Mater. Interfaces* **2015**, *7*, 980−988.
(6) Kong, D.; Cha, J. J.; Wang, H.; Lee, H. R.; Cui, Y. First-Row Transition Metal Dichalcogenide Catalysts for Hydrogen Evolution Reaction. *Energy Environ. Sci.* **2013**, *6*, 3553−3558.
(7) Lv, R.; Robinson, J. A.; Schaak, R. E.; Sun, D.; Sun, Y. F.; Mallouk, T. E.; Terrones, M. Transition Metal Dichalcogenides and Beyond: Synthesis, Properties, and Applications of Single-and Few-Layer Nanosheets. *Acc. Chem. Res.* **2015**, *48*, 56−64.
(8) Chen, W.-F.; Muckerman, J. T.; Fujita, E. Recent Developments in Transition Metal Carbides and Nitrides as Hydrogen Evolution Electrocatalysts. *Chem. Commun.* **2013**, *49*, 8896−8909.
(9) Youn, D. H.; Han, S.; Kim, J. Y.; Kim, J. Y.; Park, H.; Choi, S. H.; Lee, J. S. Highly Active and Stable Hydrogen Evolution Electrocatalysts Based on Molybdenum Compounds on Carbon Nanotube−Graphene Hybrid Support. *ACS Nano* **2014**, *8*, 5164−5173.
(10) Liu, Y. P.; Yu, G. T.; Li, G. D.; Sun, Y.; Asefa, T.; Chen, W.; Zou, X. Coupling Mo_2C with Nitrogen-Rich Nanocarbon Leads to Efficient Hydrogen-Evolution Electrocatalytic Sites. *Angew. Chem., Int. Ed.* **2015**, *54*, 10752−10757.
(11) Wu, H. B.; Xia, B. Y.; Yu, L.; Yu, X.-Y.; Lou, X. W. D. Porous Molybdenum Carbide Nano-Octahedrons Synthesized via Confined Carburization in Metal-Organic Frameworks for Efficient Hydrogen Production. *Nat. Commun.* **2015**, *6*, 6512.
(12) Liao, L.; Wang, S. N.; Xiao, J. J.; Bian, X. J.; Zhang, Y. H.; Scanlon, M. D.; Hu, X.; Tang, Y.; Liu, B. H.; Girault, H. H. a Nanoporous Molybdenum Carbide Nanowire as an Electrocatalyst for Hydrogen Evolution Reaction. *Energy Environ. Sci.* **2014**, *7*, 387−392.
(13) Ge, C. J.; Jiang, P.; Cui, W.; Pu, Z. H.; Xing, Z. C.; Asiri, A. M.; Obaid, A. Y.; Sun, X. P.; Tian, J. Shape-Controllable Synthesis of Mo_2C Nanostructures as Hydrogen Evolution Reaction Electrocatalysts with High Activity. *Electrochim. Acta* **2014**, *134*, 182−186.
(14) Xiong, K.; Li, L.; Zhang, L.; Ding, W.; Peng, L. S.; Wang, Y.; Chen, S. G.; Tan, S. Y.; Wei, Z. D. Ni-doped Mo_2C Nanowires Supported on Ni Foam as a Binder-Free Electrode for Enhancing the Hydrogen Evolution Performance. *J. Mater. Chem. A* **2015**, *3*, 1863−1867.
(15) Cui, W.; Cheng, N. Y.; Liu, Q.; Ge, C. J.; Asiri, A. M.; Sun, X. P. Mo_2C Nanoparticles Decorated Graphitic Carbon Sheets: Biopolymer-Derived Solid-State Synthesis and Application as an Efficient Electrocatalyst for Hydrogen Generation. *ACS Catal.* **2014**, *4*, 2658−2661.
(16) Zhang, J.; Meng, X.; Zhao, J. H.; Zhu, Z. P. Construction of a Mo_xC/Ni Network Electrode with Low Overpotential for Hydrogen Generation. *ChemCatChem* **2014**, *6*, 2059−2064.
(17) Kwak, W.-J.; Lau, K. C.; Shin, C.-D.; Amine, K.; Curtiss, L. A.; Sun, Y.-K. a Mo_2C/Carbon Nanotube Composite Cathode for Lithium−Oxygen Batteries with High Energy Efficiency and Long Cycle Life. *ACS Nano* **2015**, *9*, 4129−4137.
(18) Zhang, K.; Li, C. Y.; Zhao, Y.; Yu, X. B.; Chen, Y. J. One-Dimensional Mo_2C−Amorphous Carbon Composites: High-Efficient and Durable Electrocatalysts for Hydrogen Generation. *Phys. Chem. Chem. Phys.* **2015**, *17*, 16609−16614.
(19) Fan, M. H.; Chen, H.; Wu, Y. Y.; Feng, L.-L.; Liu, Y. P.; Li, G.-D.; Zou, X. X. Growth of Molybdenum Carbide Micro-islands on Carbon Cloth toward Binder-Free Cathodes for Efficient Hydrogen Evolution Reaction. *J. Mater. Chem. A* **2015**, *3*, 16320−16326.
(20) Higginbotham, A. L.; Kosynkin, D. V.; Sinitskii, A.; Sun, Z. Z.; Tour, J. M. Lower-Defect Graphene Oxide Nanoribbons from Multiwalled Carbon Nanotubes. *ACS Nano* **2010**, *4*, 2059−2069.
(21) Yang, Z. B.; Liu, M. K.; Zhang, C.; Tjiu, W. W.; Liu, T. X.; Peng, H. S. Carbon Nanotubes Bridged with Graphene Nanoribbons and Their Use in High-Efficiency Dye-Sensitized Solar Cells. *Angew. Chem., Int. Ed.* **2013**, *52*, 3996−3999.
(22) Liu, M. K.; Song, Y. F.; He, S. X.; Tjiu, W. W.; Pan, J. S.; Xia, Y.-Y.; Liu, T. X. Nitrogen-Doped Graphene Nanoribbons as Efficient Metal-Free Electrocatalysts for Oxygen Reduction. *ACS Appl. Mater. Interfaces* **2014**, *6*, 4214−4222.
(23) Chen, L.; Du, R.; Zhu, J. H.; Mao, Y. Y.; Xue, C.; Zhang, N.; Hou, Y. L.; Zhang, J.; Yi, T. Three-Dimensional Nitrogen-Doped Graphene Nanoribbons Aerogel as a Highly Efficient Catalyst for the Oxygen Reduction Reaction. *Small* **2015**, *11*, 1423−1429.
(24) Gu, H. H.; Zhang, L. S.; Huang, Y. P.; Zhang, Y. F.; Fan, W.; Liu, T. X. Quasi-One-Dimensional Graphene Nanoribbon-Supported MoS_2 Nanosheets for Enhanced Hydrogen Evolution Reaction. *RSC Adv.* **2016**, *6*, 13757−13765.
(25) Pan, L. F.; Li, Y. H.; Yang, S.; Liu, P. F.; Yu, M. Q.; Yang, H. G. Molybdenum Carbide Stabilized on Graphene with High Electrocatalytic Activity for Hydrogen Evolution Reaction. *Chem. Commun.* **2014**, *50*, 13135−13137.
(26) Kosynkin, D. V.; Higginbotham, A. L.; Sinitskii, A.; Lomeda, J. R.; Dimiev, A.; Price, B. K.; Tour, J. M. Longitudinal Unzipping of Carbon Nanotubes to Form Graphene Nanoribbons. *Nature* **2009**, *458*, 872−876.
(27) Huang, Y. P.; Miao, Y. E.; Zhang, L. S.; Tjiu, W. W.; Pan, J. S.; Liu, T. X. Synthesis of Few-Layered MoS_2 Nanosheet-Coated Electrospun SnO_2 Nanotube Heterostructures for Enhanced Hydrogen Evolution Reaction. *Nanoscale* **2014**, *6*, 10673−10679.
(28) Tang, C. Y.; Sun, A. K.; Xu, Y. S.; Wu, Z. Z.; Wang, D. Z. High Specific Surface Area Mo_2C Nanoparticles as an Efficient Electrocatalyst for Hydrogen Evolution. *J. Power Sources* **2015**, *296*, 18−22.
(29) Ma, F. X.; Wu, H. B.; Xia, B. Y.; Xu, C. Y.; Lou, X. W. D. Hierarchical β-Mo_2C Nanotubes Organized by Ultrathin Nanosheets as a Highly Efficient Electrocatalyst for Hydrogen Production. *Angew. Chem., Int. Ed.* **2015**, *54*, 15395−15399.
(30) Wan, C.; Regmi, Y. N.; Leonard, B. M. Multiple Phases of Molybdenum Carbide as Electrocatalysts for the Hydrogen Evolution Reaction. *Angew. Chem.* **2014**, *126*, 6525−6528.
(31) Zhu, Y. P.; Wang, S. F.; Zhong, Y. J.; Cai, R.; Li, L.; Shao, Z. P. Facile Synthesis of a MoO_2−Mo_2C−C Composite and Its Application as Favorable Anode Material for Lithium-ion Batteries. *J. Power Sources* **2016**, *307*, 552−560.
(32) Wang, B.; Wang, G.; Wang, H. Hybrids of Mo_2C Nanoparticles Anchored on Graphene Sheets as Anode Materials for High Performance Lithium-ion Batteries. *J. Mater. Chem. A* **2015**, *3*, 17403−17411.
(33) Awadallah-F, A.; Mostafa, T. B. Effect of Functionalized Multi-walled Carbon Nanotubes with Poly(N-vinyl pyrrolidone-co-2-acrylamido-2-methyl-1-propanesulfonic acid) on the Release of Tramadol Hydrochloride. *Chin. J. Polym. Sci.* **2015**, *33*, 376−385.

DOI: 10.1021/acssuschemeng.6b00859
ACS Sustainable Chem. Eng. 2016, 4, 6313−6321

(34) Li, Y. X.; Gao, Y.; Yang, C.; Wang, Z. Q.; Xue, G. Facile and Controllable Assembly of Multiwalled Carbon Nanotubes on Polystyrene Microspheres. *Chin. J. Polym. Sci.* **2014**, *32*, 711−717.
(35) Wang, D.-Y.; Gong, M.; Chou, H.-L.; Pan, C.-J.; Chen, H.-A.; Wu, Y.; Lin, M.-C.; Guan, M.; Yang, J.; Chen, C.-W. Highly Active and Stable Hybrid Catalyst of Cobalt-doped FeS_2 Nanosheets−Carbon Nanotubes for Hydrogen Evolution Reaction. *J. Am. Chem. Soc.* **2015**, *137*, 1587−1592.
(36) Cabán-Acevedo, M.; Stone, M. L.; Schmidt, J.; Thomas, J. G.; Ding, Q.; Chang, H.-C.; Tsai, M.-L.; He, J.-H.; Jin, S. Efficient Hydrogen Evolution Catalysis Using Ternary Pyrite-type Cobalt Phosphosulphide. *Nat. Mater.* **2015**, *14*, 1245−1251.
(37) Kornienko, N.; Resasco, J.; Becknell, N.; Jiang, C.-M.; Liu, Y.-S.; Nie, K.; Sun, X.; Guo, J.; Leone, S. R.; Yang, P. Operando Spectroscopic Analysis of an Amorphous Cobalt Sulfide Hydrogen Eevolution Electrocatalyst. *J. Am. Chem. Soc.* **2015**, *137*, 7448−7455.
(38) Kibsgaard, J.; Jaramillo, T. F. Molybdenum Phosphosulfide: an Active, Acid-Stable, Earth-Abundant Catalyst for the Hydrogen Evolution Reaction. *Angew. Chem., Int. Ed.* **2014**, *53*, 14433−14437.
(39) Ma, L.; Ting, L. R. L.; Molinari, V.; Giordano, C.; Yeo, B. S. Efficient Hydrogen Evolution Reaction Catalyzed by Molybdenum Carbide and Molybdenum Nitride Nanocatalysts Synthesized via the Urea Glass Route. *J. Mater. Chem. A* **2015**, *3*, 8361−8368.
(40) Vrubel, H.; Hu, X. Molybdenum Boride and Carbide Catalyze Hydrogen Evolution in Both Acidic and Basic Solutions. *Angew. Chem.* **2012**, *124*, 12875−12878.
(41) Chen, P.; Xu, K.; Tao, S.; Zhou, T.; Tong, Y.; Ding, H.; Zhang, L.; Chu, W.; Wu, C.; Xie, Y. Phase-Transformation Engineering in Cobalt Diselenide Realizing Enhanced Catalytic Activity for Hydrogen Evolution in an Alkaline Medium. *Adv. Mater.* **2016**, *28*, 7527.
(42) Tian, J.; Liu, Q.; Cheng, N.; Asiri, A. M.; Sun, X. Self-Supported Cu_3P Nanowire Arrays as an Integrated High-Performance Three-Dimensional Cathode for Generating Hydrogen from Water. *Angew. Chem., Int. Ed.* **2014**, *53*, 9577−9581.
(43) McKone, J. R.; Sadtler, B. F.; Werlang, C. A.; Lewis, N. S.; Gray, H. B. Ni−Mo Nanopowders for Efficient Electrochemical Hydrogen Evolution. *ACS Catal.* **2013**, *3*, 166−169.
(44) Weidman, M. C.; Esposito, D. V.; Hsu, Y.-C.; Chen, J. G. Comparison of Electrochemical Stability of Transition Metal Carbides (WC, W_2C, Mo_2C) over a Wide pH Range. *J. Power Sources* **2012**, *202*, 11−17.

DOI: 10.1021/acssuschemeng.6b00859
ACS Sustainable Chem. Eng. 2016, 4, 6313−6321